

This is an Open Access document downloaded from ORCA, Cardiff University's institutional repository:<https://orca.cardiff.ac.uk/id/eprint/136528/>

This is the author's version of a work that was submitted to / accepted for publication.

Citation for final published version:

An, Ni, Zagorščak, Renato , Thomas, Hywel Rhys and Gao, Wu 2021. A numerical investigation into the environmental impact of underground coal gasification technology based on a coupled thermal-hydro-chemical model. *Journal of Cleaner Production* 290 , 125181. 10.1016/j.jclepro.2020.125181

Publishers page: <http://dx.doi.org/10.1016/j.jclepro.2020.125181>

Please note:

Changes made as a result of publishing processes such as copy-editing, formatting and page numbers may not be reflected in this version. For the definitive version of this publication, please refer to the published source. You are advised to consult the publisher's version if you wish to cite this paper.

This version is being made available in accordance with publisher policies. See <http://orca.cf.ac.uk/policies.html> for usage policies. Copyright and moral rights for publications made available in ORCA are retained by the copyright holders.



A numerical investigation into the environmental impact of underground coal gasification  
technology based on a coupled thermal-hydro-chemical model

Ni An<sup>\*</sup>, Renato Zagorščak, Hywel Rhys Thomas, Wu Gao

Geoenvironmental Research Centre (GRC), School of Engineering, Cardiff University, The  
Queen's Buildings, The Parade, Cardiff, CF24 3AA.

**Abstract:** This study aims to improve the understanding of the potential environmental impact of the underground coal gasification (UCG) process based on a numerical investigation of the gaseous and dissolved chemicals' transport in the strata surrounding the UCG reactor. A coupled thermal-hydro-chemical (THC) model in the framework of COMPASS code is employed and further developed for this purpose. The model is compared against analytical solutions in the verification process and applied against a former UCG trial (Hoe Creek UCG programme) for validation purpose. The numerical model is then applied to investigate the potential environmental impact of UCG in three different geological materials (sandstone, coal, and shale) in two steps: the potential gas propagation during UCG process and the solute transport in UCG decommissioning stage. The results indicate that the gas propagation is limited to a near-cavity area in geological strata with low permeability and high air entry value such as shale, which is mainly attributed to the dry zone generated by the high temperature, while a larger gas plume is observed for materials with poor water retention characteristics, such as coal and sandstone. Besides, the gas propagation is retarded to some extent due to the reducing effect of high pressure on gas diffusion. The propagation of dissolved chemicals via diffusion is limited to near-cavity areas, i.e. 2 m, in three studied materials after 10 years. Based on the improved understanding of the various chemicals' migration in

different materials, by selecting the target coal seam surrounded by strata layers with high air entry value and low permeability, the gas losses from the reactor during the UCG reactor operation stage can be minimized and the potential negative environmental impact of ash leaching and solute propagation in UCG decommissioning stage can be avoided. This work also provides further insight and suggestions into the importance of investigating the adsorption capacities of different geological media to evaluate their performance as a natural cleaning system.

**Keywords:** Underground coal gasification (UCG); Environmental impact; Coupled thermal-hydro-chemical model; High temperature/pressure; Gas/solute propagation

## 1. Introduction

Underground coal gasification (UCG) is the process of converting a coal seam into synthesis gas in-situ by injecting sufficient air/oxygen/steam mixture to gasify the coal at a high temperature. The purpose of UCG is to access and harvest the energy contained within the solid fuel underground, without applying conventional mining methods. Various articles and studies indicate that UCG is a technically feasible and economically viable method to utilize the deep coal resource, which has attracted an ongoing interest of several nations with abundant coal resources, such as China, India, South Africa, Australia, Pakistan, and Poland, etc. to develop and employ this technology (Attwood et al., 2003; Shafirovich and Varma, 2009; Bhutto et al., 2013; Khadse, 2015; Khan et al., 2015; Wen et al., 2016; Wiatowski et al., 2016; Xin et al., 2017; Perkins, 2018; Xie et al., 2020). UCG has the potential to contribute positively to the environmental perspective of the unmined deep coal seams owing to no discharge of tailings and reduced emission of sulfur, ash, mercury, and tar. However, the gasification reactor can also be a possible source of both gaseous and liquid contaminants based on the site observations (Figure 1) ( Humenick and Maitox, 1977; Campbell et al., 1978; Dalton and Campbell, 1978; Stuermer et al., 1982; Liu et al., 2007; Kapusta

et al., 2013; Imran et al., 2014; Man et al., 2014). Hence, the potential environmental concerns related to UCG need to be addressed and understood to allow for its commercialization.

The environmental concerns have been comprehensively reviewed by Imran et al. (2014), including the potential subsidence, the escape of product gases into the air and surface soil, and the change of groundwater quality, etc. The surface subsidence occurs in UCG as a result of the coal consumption in underground layer formation, similar to the effects caused by conventional mining. This was observed in many UCG projects operated at shallow depths and in moderate to thick coal seams (Creedy et al., 2001; Derbin et al., 2015; Mao, 2016; Burton et al., 2017). Burton et al. (2017) suggested that the reactor pressure should be equal or below the surrounding hydrostatic pressure during the gasification process, to minimize the escape of the syngas to the surrounding strata. However, in the field test of El Tremedal UCG site, gas losses were observed by Chappell and Mostade (1998) when high reactor pressure was applied. Overall, it is common for between 5% and 25% of the gas to be lost from the underground gasifier (Campbell, 2016). Imran et al. (2014) also concluded that groundwater quality change is generally considered as the most significant environmental risk related to UCG operations. A comprehensive site investigation of the groundwater quality near Hoe Creek UCG site was conducted by Campbell et al. (1978). The type, amount and fate of the UCG produced contaminants were determined, revealing that a significantly increased concentration of organic chemicals, particularly phenols, were just outside the reactor boundary and the observed inorganic species principally arise from ash leachate. Moreover, it was observed that all detectable contaminants decreased significantly in concentration with distance. The adsorption of UCG organics by coal, char and ash were studied Humenick et al. (1987) and the metal species adsorption by coal and char were examined by Strugała-Wilczek et al. (2020), presenting the potential of the UCG solid materials to perform as a natural adsorbent. Kapusta et

al. (2013) investigated the wide range of organic and inorganic contaminants for the experimental mine “Barbara” in Poland and revealed that the main source of toxic trace elements is the post-gasification residuals. No chemical hazards were identified on the site surface, proving the importance of an appropriate site selection and fair process control in shallow coal seams. The gas migration towards the surface was prevented but the UCG-induced thermal effects on the surface were observed. Other field investigations and laboratory experimental tests targeting on different coals in different regions were also carried out (Dalton and Campbell, 1978; Strugała-Wilczek and Stańczyk, 2016; Wiatowski et al., 2016; Sadasivam et al., 2020). In the above-mentioned studies, the typical chemicals include organic species, such as phenols, benzene, minor components such as PAHs and heterocyclics, and inorganic species, cations ( $\text{Na}^+$ ,  $\text{K}^+$ ,  $\text{Mg}^{2+}$ ,  $\text{NH}_4^+$ , etc.) and anions ( $\text{SO}_4^{2-}$ ,  $\text{HCO}_3^-$ ,  $\text{Cl}^-$ , etc.). The organic species are mainly generated during the gasification process due to the pyrolysis of the coal seam. Meanwhile, the produced coal ash and char are left in the cavity and remain largely isolated from the groundwater. However, the surrounding water starts to invade the cavity after the completion of the coal gasification process. As the cavity cools and fills with water, the inorganic species from coal ash and residues may be leached out. The types and concentrations of these chemical species vary depending on coal and ash compositions, gasifier temperatures, and natural water quality. The fate of these chemical species may be affected by temperature, adsorption-desorption, precipitation-dissolution, and ion-exchange reactions, etc. (Campbell et al., 1978; Kapusta et al., 2013).

As having a fully instrumented UCG trial with comprehensive data extraction is challenging and expensive, computational modelling offers an inexpensive way for predicting the complex interaction of various processes involved during and beyond the UCG operation. The numerical method provides the possibility to estimate the spatial and temporal variations of chemicals in the

surrounding region of UCG reactor (Yang and Zhang, 2009; Soukup et al., 2015). Yang and Zhang (2009) carried out a numerical simulation of the transport process for the solute in the UCG panel, presenting the main solute transport mechanisms. They indicated that the influence range of temperature field expanded, the gradient of groundwater pressure decreased, and the migration velocity of dissolved chemicals increased as the gasification progressed. Soukup et al. (2015) conducted numerical modelling of contaminant migration and found that the key transport parameters, such as porosity, pore diameter, and tortuosity, play a major role in the propagation of gaseous chemicals compared with physical characteristics-pressure and temperature. In general, migration rates of UCG-related chemicals in the liquid phase are significantly slower compared with the gaseous phase. However, the comprehensive investigation of both gaseous and dissolved chemicals propagation in the strata surrounding the UCG reactor remains scarce.

The aim of this study is to provide an improved understanding of the potential environmental impact of UCG based on a numerical investigation of the gaseous and dissolved chemicals' transport in the surrounding strata. A coupled thermal-hydro-chemical (THC) model in the framework of COMPASS code is employed and further developed for UCG application. The model is compared against analytical solutions in the verification process for the study purpose. It is then applied against a former UCG trial (Hoe Creek UCG programme) for validation purpose based on two series of laboratory experiments designed to deal with the release and migration of chemical species produced during UCG process. The numerical model is then applied to investigate the potential environmental impact of UCG in three geological materials (sandstone, coal and shale) in two steps: the potential gas propagation during the UCG process and the solute transport in the UCG decommissioning stage.

## 2. Numerical method

### 2.1 Governing equations for chemical transport

An understanding of the physical processes involved in multiphase flows in strata surrounding the UCG reactor is required to accurately investigate the transport of various chemicals. For this work, few assumptions are made herein. Vapour flow mainly participates in the reaction of the coal gasification process, which is outside the scope of this work. Thereby, the transport of liquid water, heat, and chemicals (gaseous and dissolved) are considered herein. The studied zone is assumed to be homogeneous. The multiphase flows are introduced as follows:

#### 2.2.1 Liquid flow

The governing equation of liquid flow can be described by:

$$\frac{\partial(\rho_l \theta_l)}{\partial t} = -\nabla \rho_l V_l \quad (1)$$

Where,  $\rho_l$  ( $\text{kg/m}^3$ ) represents the liquid density;  $\theta_l$  is the water content;  $V_l$  (m/s) is the liquid velocity, which is estimated based on Darcy's law:

$$V_l = -K_w \nabla(\varphi + y) \quad (2)$$

where  $K_w$  (m/s) is the hydraulic conductivity;  $\varphi$  (m) is the matric suction head;  $y$  (m) is the elevation above a nominal datum.

#### 2.2.2 Heat flow

The governing equation of heat flow is expressed by:

$$\frac{\partial[H_c(T - T_r)]}{\partial t} = -\nabla[-\lambda_T \nabla T + (C_{pl}\rho_l V_l + C_{pg}\rho_g V_g)(T - T_r)] \quad (3)$$

Where,  $H_c$  and  $\lambda$  are the specific heat capacity ( $J/(m^3 \cdot K)$ ) and the thermal conductivity ( $W/(m \cdot K)$ ) of the studied porous media, respectively;  $T$  and  $T_0$  are the temperature and the reference temperature (K);  $C_{pl}$  and  $C_{pg}$  are the specific heat capacity of liquid and air ( $J/(kg \cdot K)$ ), respectively;  $\rho_g$  ( $kg/m^3$ ) represents the gas density;  $V_g$  is the gas velocity and can be defined by a generalized Darcy's law:

$$V_g = -K_g \nabla P_g / \rho_g g \quad (4)$$

Where,  $K_g$  (m/s) is the gas conductivity;  $P_g$  (Pa) is the gas pressure. In this study, heat transport includes conduction and convection, as presented by the first and second terms in the right-hand side of equation (3). Latent heat is not considered due to the neglect of vapour flow in this work.

### 2.2.3 Multichemical flow

The gas and solute propagation in different porous media is to be investigated during and after the UCG process, respectively. The coal gasification process is generally performed under high pressure and temperature. Generally, both gas diffusion and advection contribute to the transport of gaseous products from the reaction zone into both the production well and the surrounding strata. During the UCG decommissioning stage, the cavity is refilled with water, favouring the propagation of dissolved chemicals leached from ash/tar residues in the cavity. In this part, the transport of both gaseous and dissolved chemicals involves three main mechanisms: advection, diffusion, and adsorption.

Ideal-gas law is applied in this study for simplification. The governing equation of multicomponent chemical flow in gaseous and liquid phases are given by:

$$\frac{\partial(c_g^i n S_g)}{\partial t} = \nabla[D_g^i \nabla c_g^i] - \nabla[c_g^i V_g] + s_g^i \quad (5)$$

$$\frac{\partial(c_d^i n S_l)}{\partial t} = \nabla[D_d^i \nabla c_d^i] - \nabla[c_d^i V_l] + s_d^i \quad (6)$$

Where,  $c_g^i$  and  $c_d^i$  represent the  $i^{\text{th}}$  gaseous ( $\text{mol}/\text{m}^3$ ) and dissolved (ppm) chemical concentration, respectively;  $n$  is the porosity;  $S_g$  and  $S_l$  are the degree of saturation in gas and liquid phases, respectively;  $D_g^i$  and  $D_d^i$  represent the diffusion coefficient ( $\text{m}^2/\text{s}$ ) of the  $i^{\text{th}}$  gaseous and dissolved chemical species, respectively;  $s_g^i$  and  $s_d^i$  represent the sink/source term in the gaseous and dissolved chemical transports. Specifically, the first, second, and third terms in the right-hand side of equations (5) and (6) represent the diffusion, advection, and reactive/adsorption terms in multichemical flows. When adsorption/desorption is considered as the sink/source term, they can be expressed by:

$$s_j^i = \frac{\partial \rho_s V_E}{\partial t} \quad (7)$$

Where,  $j$  represents the chemicals in gaseous ( $g$ ) and dissolved ( $d$ ) phases;  $\rho_s$  is the bulk density of porous media;  $V_E$  is the standard gas/solute volume adsorbed per unit mass of porous media.

Considering the high-temperature environment generated by the coal gasification process, the effect of temperature on the gas and solute propagation is also considered in this study. Gas diffusion coefficients decrease with rising pressure and increase with temperature as indicated by Pillalamarry et al. (2011), Pone et al. (2009), Wang and Liu (2016). Thereby, to estimate such behaviour, the Chapman-Enskog theory was employed to calculate the value of gas diffusion coefficient affected by both temperature and pressure (Poling et al., 2001):

$$D_g^i = \frac{2.66 \times 10^{-12} T^{3/2}}{P_g M_{AB}^{1/2} \sigma_{AB}^2 \Omega_D} \quad (8)$$

Where,  $M_{AB}$  is the molecular weights;  $\sigma_{AB}$  is the characteristic length ( $\text{\AA}$ );  $\Omega_D$  is the diffusion collision integral. Equation (8) indicates that temperature and pressure have the opposite effect on the syngas diffusion in the porous media.

Moreover, the value of solute diffusion coefficient affected by temperature is estimated by Stokes-Einstein equation (0~643.15 K) following the hydrodynamic theory (Bird et al., 1960; Gainer and Metzner, 1965; Poling et al., 2001):

$$D_d^i = \frac{kT}{6\pi\mu r} \quad (9)$$

Where,  $k$  is the Boltzmann's constant;  $r$  is the radius of the spherical particle;  $\mu$  represents the water viscosity (0~643.15 K), which is estimated by:

$$\mu = 2.414 \times 10^{-5} \times 10^{247.8/(T-140)} \quad (10)$$

Equation (9) indicates that the diffusion coefficient of the dissolved chemical presents an increasing tendency as the temperature goes up.

## ***2.2 The developed numerical method and code introduction***

In this study, the coupled heat, water, and multi-component chemical transfer in surrounding strata is analyzed with consideration of the coal gasification process and decommissioning stage using code COMPASS, developed at Cardiff University's Geoenvironmental Research Centre. The COMPASS code is a coupled thermo-hydro-chemical-mechanical (THCM) model with a

background of high-performance simulations of three-dimensional multiphase, multicomponent reactive transport in geomaterials and high applicability in a various range of geo-environmental and geo-energy problems (Thomas, 1985; Thomas et al., 1998, 2009). Thereby, the coupled thermal-hydro-chemical (THC) framework of the COMPASS code is adopted and further developed herein to study the transport of chemicals in gaseous and aqueous phases involved in UCG process. It involves the inclusion of the constitutive relationship that describes the temperature or pressure dependent material parameter and key processes. Specifically, the heat capacity and thermal conductivity of various rocks are introduced as temperature-dependent constitutive relationships (Kosowska-Golachowska et al., 2014; Otto and Kempka, 2015; Tang et al., 2015; Zagorščak et al., 2019). Furthermore, geochemical reactions are considered via the equilibrium/kinetic adsorption/desorption module in COMPASS (Hosking et al., 2018).

Besides, the UCG process is assumed to be conducted following the best practice guidelines, which is keeping the reactor pressure below hydrostatic (Burton et al., 2017). It is also assumed that the disturbed zone by UCG process does not extend sufficiently far that it provides a direct permeable connection between the reactor zone and any overlying aquifers. Hence, the thermally/mechanically induced strata change along with cavity creation, which means the alteration of the strata properties (Jiang et al., 2020), i.e. porosity, permeability, and soil water retention characteristics, are not included in this work.

The highly coupled nature of the COMPASS framework requires a simultaneous solution of the governing equations and the non-linearity of the problems considered requires an iterative technique to achieve a converged solution. Hence, the finite element method (FEM) via the Galerkin weighted residual method is employed to spatially discretize the system of equations, whereas the finite difference method (FDM) via an implicit mid-interval backward difference

algorithm is applied to achieve temporal discretization. A sequential (time-splitting) approach is employed to solve the chemical transport and reaction equations. A pre- and post-processing package (GiD) is linked to the code. This allows mesh generation, definitions of initial and boundary conditions and material parameters, and processing of the results in a user-friendly framework.

### **3. Model verification**

The THCM model of the COMPASS code has been extensively verified, validated, and applied for a range of geo-environmental and geo-energy applications ( Thomas, 1985; Thomas et al., 1998, 2009; Hosking et al., 2018). For instance, the thermal aspects of the model have been verified against analytical solutions and validated against experimental data on heat propagation in a rock (Zagorščak et al., 2017). Moreover, the multiphase flow, considering the evolution of the degree of saturation as water and high-pressure ideal gas flow in a partially saturated single porosity medium has been verified (Hosking et al., 2018). For model application in the area of UCG, few verification exercises in terms of multichemical flows are detailed here to acquire the confidence of the developed model for the predictive purpose. The model is compared against analytical solutions in the verification process.

#### ***3.1 Diffusion and convection of dissolved chemicals***

For the case of one-dimensional transport of a single solute component in a homogenous isotropic porous medium, the advection-diffusion equation can be described by:

$$\frac{\partial(c_d^i n S_l)}{\partial t} = D_d^i \frac{\partial^2 c_d^i}{\partial x^2} - V_l \frac{\partial c_d^i}{\partial x} \quad (11)$$

Where,  $t$  is time and  $x$  is the distance in the flow direction. Ogata and Banks (1961) presented an analytical solution to equation (8) considering the following initial and boundary conditions:

$$C_d(x, 0) = C_i \quad (12)$$

$$C_d(0, t) = C_0 \quad (13)$$

$$\frac{\partial C_d(\infty, t)}{\partial t} = 0.0 \quad (14)$$

Where,  $C_i$  is the initial concentration and  $C_0$  represents the concentration at the source or at  $x = 0.0$ .

The analytical solution was given as follows:

$$C_d(x, t) = C_i + \frac{C_0 - C_i}{2} \left[ \operatorname{erfc} \left\{ \frac{x - V_l t}{2(Dt)^{0.5}} \right\} + \exp \left( \frac{V_l x}{D} \right) \cdot \operatorname{erfc} \left\{ \frac{x + V_l t}{2(Dt)^{0.5}} \right\} \right] \quad (15)$$

In this exercise, a 10.0 m by 0.2 m saturated sandstone sample with a porosity of 0.25 was used to investigate such behaviour. The sample domain is discretized into 50 equally sized quadrilateral elements. The simulation is carried out for 1000 hours. The average linear liquid velocity  $V_l$  is set as  $1.0 \times 10^{-6}$  m/s. The diffusion coefficient  $D$  ( $\text{m}^2/\text{s}$ ) is set as  $1.0 \times 10^{-7}$   $\text{m}^2/\text{s}$ . The initial chemical concentration is assumed as zero. At the left boundary, *i.e.*  $x = 0$ , solute boundary condition is prescribed for a constant source concentration of 10.0 mg/L. At the right boundary, *i.e.*  $x = 10.0$  m, no chemical flux is applied.

The concentration profiles for advective-diffusive flow in the saturated sandstone sample have been obtained using the analytical solution and numerical model, as shown in Figure 2. A good

agreement between the analytical and numerical modelling results can be observed in the solute concentration profile after 1000 hours (Figure 2a) and the solute concentration evolutions at point (0.5, 0.1) (Figure 2b). It indicates that the diffusion and advection transport mechanisms have been correctly implemented in the transport module of COMPASS. The minor difference between the analytical and numerical concentration results is mainly attributed to the right boundary condition: zero-flux was applied at the right boundary ( $x = 10.0$  m) for simulation and the far-field boundary ( $x = \infty$ ) for analytical calculation.

### **3.2 Reactive transport**

The gas flow considering diffusion, advection, and adsorption in porous media is described by equation (5). When the adsorption process is described by the Langmuir isotherm model, the adsorbed gas volume can be given as:

$$V_E = V_L \frac{P}{P + P_L} \quad (16)$$

Where,  $V_L$  is the Langmuir's volume (mol/kg),  $P$  and  $P_L$  are the gas pressure and Langmuir's pressure (Pa). The theoretical derivation conducted by Wu et al. (2014) provides the approximate analytical solution:

$$P^2(r, t) = P_i^2 - \frac{\mu Q_m}{2\pi k h \beta} E_i \left( -\frac{r^2}{4At} \right) \quad (17)$$

Where,  $P$  is the transient pressure (Pa). Other details about the analytical solution derivation are not repeated herein, which can be found in Wu et al. (1998, 2014).

A 1D radial uniform region is used to study the transient gas (CO<sub>2</sub>) flow with and without considering adsorption in a porous media with a porosity of 0.25. The initial gas pressure of  $1.0 \times 10^5$  Pa is assumed to be uniform throughout the overall region. A constant gas mass injection rate of  $1.0 \times 10^5$  kg/s is imposed at the well boundary. Langmuir model is applied herein to describe the equilibrium adsorption process. The Langmuir volume (mol/kg) and pressure (Pa) are 0.49 and  $2.83 \times 10^6$ , respectively.

The gas concentration profiles after 1 day obtained using the analytical solution and numerical model are presented in Figure 3. An excellent agreement between the analytical and COMPASS result can be observed in both cases: with and without adsorption. Moreover, the results indicate that the gas propagation in the case considering adsorption is slower compared to the results without adsorption, reflecting the retardation influence of the adsorption.

#### **4. Model validation against UCG related small-scale experiments (Hoe-creek I site)**

The COMPASS code is applied against available literature data on former UCG trials for the validation purpose. Hoe Creek UCG programme conducted by the Lawrence Livermore National Laboratory (LLNL), which was widely reported in literature (Campbell et al., 1978; Dalton and Campbell, 1978) was used herein. Two series of laboratory experiments were designed by Dalton and Campbell (1978) to deal with the release and migration of dissolved chemicals produced during UCG process. The first test was a leaching test for coal ash samples, providing a quantitative evaluation of released chemicals from coal ash left underground. The second one was designed to investigate the transport of phenolic materials and saline solution through the coal stratum surrounding the UCG cavity, revealing the strong adsorption of phenol by the coal. The integrated

experimental set up is presented in Figure 4. The experimental results are used herein for the model validation in terms of ash leaching and solute transport in strata adjacent to the UCG reactor.

#### ***4.1 Ash leaching test***

A 0.02 m × 0.1 m leaching column was filled with approximately 50 cm<sup>3</sup> of water and approximately 10 g of heat-treated ash sample to investigate the leaching process (Dalton and Campbell, 1978). Ca<sup>2+</sup> is studied herein as the principal species identified in the leachate. Based on the back analysis, the average water flux in the leaching column is assumed to be 3.0×10<sup>-7</sup> m/s, slightly lower than the applied water volumetric flow rates (10 cm<sup>3</sup>/hr) through the 1000 °C heated ash sample. The initial Ca<sup>2+</sup> concentration is calculated based on the maximum leachate mass, as 9.88 mg/L. Based on Dalton and Campbell (1978), the porosity of the material is taken as 0.1 and Ca<sup>2+</sup> diffusion coefficient as 5.5×10<sup>-10</sup> m<sup>2</sup>/s. The simulation is carried out for 85 hours, which corresponds to the duration of collecting the maximum leachate mass. The porous medium is considered as saturated during the studied period.

Based on the variations of residual Ca<sup>2+</sup> concentration in the studied domain calculated by COMPASS code, the leachate mass evolution of Ca<sup>2+</sup> is estimated. Figure 5 presents a good agreement between the measured and calculated result of Ca<sup>2+</sup> leachate mass, indicating that the leaching process of the heat-treated ash sample has been properly simulated with the parameters considered.

#### ***4.2 Chemical transport experiments***

In the chemical transport experiments, a plexiglass column (1.52 m × 0.1 m) was packed with coal particles approximately 0.007 m in diameter, backfilled with water using a vacuum and flushed with NaBr and phenol solution, respectively (Dalton and Campbell, 1978). Solute samples were

drawn from each port using a disposable syringe, to measure the solute concentrations at different fixed points along the length of the coal column during the experiment. Following Dalton and Campbell (1978), fixed concentrations of 102.9 and 600 mg/L are applied on one side of the domain providing a constant source of chemicals for the NaBr and phenol experiments, respectively. The simulations are carried out for 350 and 700 hours in the cases of NaBr and phenol, respectively. Table 1 details the main parameters used for the validation exercises.

The concentration profiles calculated using COMPASS code agree very well with the measured results, for both NaBr (Figure 6a) and phenol (Figure 6b). Especially, the results indicate that coal has stronger adsorption of phenol than NaBr, retarding the propagation of phenol significantly within the studied coal layer. Those results suggest that the reactive transport of inorganic and organic chemicals generated during the UCG process can be simulated properly by the COMPASS code.

## **5. Model application and analysis**

A comprehensive investigation of transport phenomena of the UCG related products would aid in determining the risk of possible threats to the environment. During the gasification process, the reactor pressure is generally kept below the surrounding hydrostatic pressure to minimize the loss of gaseous and liquid chemicals. However, if an outward pressure gradient and a pathway for flow (e.g. crack) appear for a short period, syngas losses can appear. Contrary to gaseous chemicals, dissolved chemicals are released into the surroundings of the georeactor especially after the termination of the UCG process (Dalton and Campbell, 1978; Liu et al., 2007). At the completion of gasification, groundwater begins to invade the gasifier. As the cavity cools and fills with water,

the residual ash is leached, leading to changes in pH and the concentration of many dissolved species.

COMPASS code is applied herein to gain an enhanced understanding of the coupled processes in the UCG reactor vicinity by performing numerical analysis to investigate gas and solute propagations in different strata during and after the UCG process. A simplified 1D domain with 30 m in length is studied with considering three different rock materials (sandstone, coal, and shale) as the porous media surrounding the UCG reactor. The detailed material parameters are listed in Table 2 (Liu and Smirnov, 2008; Ferrari et al., 2014; Parajuli et al., 2017). In particular, the soil-water retention characteristics and hydraulic conductivity variations of these three porous media are plotted in Figures 7a and 7b. Moreover, their thermal conductivities and heat capacities are considered as temperature-dependent following the work by Kosowska-Golachowska et al. (2014), Tang et al. (2015), and Zagorscak et al. (2019). The simulations are carried out for 10 days during the gasification process and 10 years in the decommissioning stage to investigate the gas and solute transport, respectively.

### ***5.1 Syngas transport during the UCG reactor operating stage***

The studied zone is assumed at a partially saturated initial condition with a degree of water saturation of 0.89 and an initial temperature of 305.15 K. The studied syngas includes CO<sub>2</sub>, CH<sub>4</sub>, H<sub>2</sub>, CO, and H<sub>2</sub>S, with different gas diffusion coefficients of  $1.15 \times 10^{-5}$ ,  $2.33 \times 10^{-5}$ ,  $1.48 \times 10^{-4}$ ,  $2.1 \times 10^{-5}$ , and  $1.28 \times 10^{-5}$  m<sup>2</sup>/s at 303.15 K. The initial gas concentration of each studied gas is assumed to be 0.1 mol/m<sup>3</sup>, while the initial porewater pressure is set as 4.8 MPa (Chappell and Mostade, 1998). The gas boundary conditions at the cavity are described by the fixed gas concentrations of syngas, composing of CO<sub>2</sub>, N<sub>2</sub>, H<sub>2</sub>, CH<sub>4</sub>, CO, C<sub>2</sub>H<sub>6</sub> and H<sub>2</sub>S with assumed molar

ratios based on in situ trial presented in Chappell and Mostade (1998) (Table 3) with a total gas concentration of  $500.68 \text{ mol/m}^3$ . It is assumed that the water pressure at the far-field boundary is kept as constant, allowing water flow outwards freely. The details of the initial and boundary conditions applied for the study of gas propagation are presented in Table 4. Specifically, the temperature at the boundary is assumed to increase linearly from 303.15 to 1273.15 K within the initial 1.3 days and then kept constant at 1273.15 K until the end of the studied period (Liu et al., 2019). The highest total gas pressure at the cavity boundary approaches to 5.3 MPa, based on the observation by Chappell and Mostade (1998). Considering the critical temperature (647.09 K) of water and the temperature limitation ( $<643.15 \text{ K}$ ) in the estimation of water viscosity, the degree of saturation in the studied zone is assumed to be equal to its residual capacity when the temperature is higher than 643.15 K, representing a dry porous medium with no mobile liquid water. To investigate the impact of adsorption on solute propagation in the strata surrounding the UCG reactor, the transport of phenol and  $\text{NH}_4^+$  species in the coal layer is studied based on the Langmuir model with the sorption parameters measured by Jabłońska (2012) and Tu et al. (2019).

Based on the methodology introduced above, the degree of saturation and heat propagation in three different materials after 10 days are plotted in Figures 8a and 8b, respectively. The gas and heat propagation alter the degree of saturation of the UCG surrounding strata. The dry front moves to around 22.7 m, 19.8 m and 1.0 m in sandstone, coal, and shale, respectively. Soil-water retention characteristics are the main drivers for such behavior observed in the three materials. Furthermore, it can be observed that the high temperature regions, i.e. higher than 500 K, in sandstone, coal, and shale are all limited up to 1 m. A small difference between the temperature profiles in different materials is mainly governed by their variations in thermal conductivities and heat capacities which are introduced as temperature-dependent in the model (Zagorščak et al., 2019).

As shown in Figure 9, the propagation distance of gases in three porous media (sandstone, coal, and shale) presents the same tendency:  $H_2 > CO_2 > CH_4 > CO > H_2S$ . Specifically, the movement of  $H_2$  is much faster than other gases due to the predominant effect of gas diffusion in gas transport (Zagorščak et al., 2019), which is closely related to the gas diffusion coefficient. The diffusion coefficient of  $H_2$  ( $1.48 \times 10^{-4} \text{ m}^2/\text{s}$ ) is approximately 10 times higher compared to other gases. Besides, the concentration gradients of  $H_2$  and  $CO_2$  are the highest amongst the gases in the domain, due to their high concentrations in the syngas, which directly contributes to differences in propagation distances. In general, the propagation distance of gases in sandstone is larger than that in coal and shale. Sandstone has higher porosity and permeability than coal and shale, allowing the gases to propagate to a further distance. Such behavior is consistent with the one observed in the El Tremedal UCG trial, which reported that gas losses from the cavity into the permeable sand layer above the target coal seam were high and caused reductions in the efficiency of the process (Chappel and Mostade, 1998). Due to the high air entry value of shale and its low permeability, it is difficult for syngas produced by coal gasification to transport in the shale layer surrounding the UCG reactor. The observed gas propagation is limited to 1.0~2.0 m in shale after 10 days, which is mainly attributed to the dry zone generated by the high temperature. In conclusion, the gas propagation in surrounding strata is dominated by the properties of various materials e.g. water retention curves, porosity, and permeability, and the produced gas component, e.g. gas diffusion coefficients and concentrations in the cavity. In terms of the strata with high air entry value and low permeability, e.g. shale, the reactor can be operated at pressures near hydrostatic to maximize the methane generation which is favorable under high pressures. As in such case the heat losses as a consequence of reduced gas transport and the evaporation of groundwater would be minimal, the gasifier efficiency would be elevated. However, the equilibrium between the hydrostatic pressure

in higher permeable rock type, e.g. sandstone, surrounding the UCG reactor and the production pressure within the reactor should be maintained to minimize any gas loss from the reactor.

Figures 10a and 10b show that the propagation of CO<sub>2</sub>, CH<sub>4</sub>, H<sub>2</sub>, and CO and H<sub>2</sub>S in coal with considering the temperature and pressure effects on the gas diffusion coefficient after 10 days, respectively. It can be observed that the transport of each gas species is retarded to some extent when those effects are considered. Based on the Chapman-Enskog theory, higher temperature can improve the gas diffusion coefficient value. However, the value of gas diffusion coefficient drops quickly as the gas pressure increases. Temperature and pressure have the opposite effect on the syngas diffusion in the surrounding strata. This change in gas diffusion coefficient with pressure and temperature is more significant for gases with high initial value of diffusion coefficient (e.g. H<sub>2</sub>), while the temperature and pressure changes have only minor impact on gases with low initial value of diffusion coefficient (e.g. CO<sub>2</sub>, CH<sub>4</sub>). Therefore, the results indicate that such effect should be included in the estimation of the gas diffusion coefficient when assessing the transport of syngas rich in H<sub>2</sub>, allowing a more accurate evaluation of the potential syngas transport in the surrounding strata. On the opposite, the impact of pressure and temperature on diffusive flow of gas produced at high pressures, which is rich in CO<sub>2</sub> and CH<sub>4</sub> (Zagorscak et al., 2020), and especially in strata with high permeability where advection is the dominant transport process, is less evident.

The impact of adsorption on gas propagation in the strata surrounding the UCG reactor has been investigated in our previous work (Zagorščak et al., 2019). The transport of CO<sub>2</sub> and CH<sub>4</sub> species in the coal layer surrounding the UCG reactor was studied in depth based on the extended Langmuir model, presenting the significant retardation effect of adsorption. High temperature favors the existence of gas in a free state rather than being absorbed by coal and the gas sorption capacity decreases as the temperature goes up (Chen et al., 2011; Krooss et al., 2002; Zhu et al., 2011).

However, the research on gas adsorption under high temperature above 353.15 K is still scarce. Considering the temperature propagation in the studied zone during the UCG reactor operation stage in a longer term, the temperature effect on the adsorption process requires to be included in the future study of gas transport. Besides, cavity formation may induce rock porosity and permeability changes close to the cavity, which might additionally affect the gas transport/losses in the surrounding strata. In conclusion, the evaluation of the potential syngas migration in coal can help in identifying the proper width of the safety pillars between the UCG reactors, avoiding the potential gas escape from one cavity to another, and minimizing the negative environmental impact of UCG.

### ***5.2 Reactive transport of dissolved chemicals during the UCG reactor decommissioning stage***

Based on the site investigation of Hoe Creek UCG project (Campbell et al., 1978), the typical dissolved species observed in UCG surrounding strata include phenol,  $\text{CN}^-$ ,  $\text{Ca}^{2+}$ ,  $\text{NH}_4^+$ ,  $\text{SO}_4^{2-}$ , etc. The diffusion coefficients of phenol,  $\text{CN}^-$ ,  $\text{Ca}^{2+}$ ,  $\text{NH}_4^+$ ,  $\text{SO}_4^{2-}$  are  $9.79 \times 10^{-10}$ ,  $1.53 \times 10^{-9}$ ,  $2.63 \times 10^{-9}$ ,  $1.95 \times 10^{-9}$  and  $1.89 \times 10^{-9}$   $\text{m}^2/\text{s}$ , respectively. The initial solute concentration is assumed as the baseline (0.1 ppm) and the degree of saturation is assumed as 0.9. Fixed concentrations of various dissolved chemicals, with equal values as initial, are assumed at the far-field boundary ( $x = 30$  m). The propagations of the dissolved chemicals are studied in three different scenarios: pure diffusion was considered in case 1, and diffusion and advection with two different hydraulic gradients/groundwater flow rates were considered in cases 2 and 3. Table 4 detailed the information of the initial and boundary conditions applied to the domain and the studied three scenarios. Moreover, some residual heat left in the cavity may affect the propagation of dissolved chemicals via diffusion as well. Therefore, in the case considering temperature effect, a constant temperature

of 643.15 K is applied at the cavity boundary during the whole studied period to reflect the worst scenario of high temperature in the cavity which may potentially persist for several years after the gasification process.

The propagation of dissolved chemicals in three different cases after 10 years are presented in Figures 11a, 11b, and 11c for three different materials: sandstone, coal, and shale. In sandstone, the dissolved chemicals move to around 2.1 m in case 1, 6.8 m in case 2, and 12.0 m in case 3, respectively. The dissolved chemicals in coal propagate to about 1.3 m in case 1, 4.2 m in case 2, and 7.5 m in case 3, respectively. The propagation of dissolved chemicals in shale is limited to 1.5 ~2.5 m in three cases. Generally, in three different materials, the dissolved chemicals move faster in case 3 than the other two cases due to the predominant effect of advection in solute transport. However, in case 1, it can be observed that the propagation of dissolved chemicals is limited to around 2 m in three porous media with considering pure diffusion in solute transport. In cases 2 and 3, the solutes propagate to a further distance in sandstone compared to that in coal and shale under the same hydraulic gradient. This is mainly attributed to the differences in permeabilities of the three porous media (sandstone > coal > shale). Especially, it is noticed that the propagation of the dissolved chemicals is limited to 2.5 m in three cases of shale after 10 years, presenting the good performance of shale as a potential natural buffer. In conclusion, the potential movement of the dissolved chemicals is significantly affected by the groundwater flow rate and the strata type in the zone surrounding the UCG cavity. In other words, it is of great importance to consider the hydrogeological and geological conditions carefully in the potential UCG site selection and to avoid the potential negative environmental impact.

The solute propagation in coal considering the temperature effect is also presented and compared with the case without considering temperature effect, as shown in Figure 12. For instance, phenol

propagation approaches 4.6 m in the case considering high temperature, further than 1.1 m when the high temperature effect is not considered, respectively. A similar phenomenon can also be identified for other dissolved chemicals. The results indicate that high temperature improves the solute propagation in the coal. An understanding of the cooling regime and the persistence of the residual heat in the cavity after UCG process would be helpful to reliably estimate the solute propagation in the surrounding strata. Nevertheless, as residual temperature can only persist for several years in the gasification cavity and the cavity will eventually become in thermal equilibrium with the surrounding environment, the impact of temperature on the transport of dissolved chemicals for the timeframes that need to be considered (>1000 years) in ensuring that the unacceptable risks to the environment will not arise, is believed to be limited.

To investigate the impact of adsorption on solute propagation in the strata surrounding the UCG reactor, the transport of phenol and  $\text{NH}_4^+$  species in the coal layer is studied based on the Langmuir model with the sorption parameters measured by Jabłońska (2012) and Tu et al. (2019), as shown in Table 5. Figures 13a and 13b indicate that the propagation of phenol and  $\text{NH}_4^+$  in the case considering adsorption is much slower compared to the results without adsorption, reflecting the significant retardation effect of the adsorption. It also suggests that more experimental work on the sorption properties of other chemicals by different rocks surrounding the UCG reactor is still required in the further investigation of UCG environmental impact.

Furthermore, some residual heat left in the cavity in the UCG decommissioning stage may also influence the adsorption process of dissolved chemicals by the strata layers. It would be beneficial to have an understanding of the non-isothermal adsorption of dissolved chemicals by different UCG surrounding strata materials. In conclusion, in the UCG decommissioning stage, the groundwater flow regime and the duration of UCG cavity cooling stage need to be estimated to

evaluate the long-term impact of UCG operation. Due to the paucity of the research on this aspect, more experimental work on adsorption of the UCG produced risky chemical species by different rocks (under different temperatures) is necessary to allow for reliable assessment of both reactive gas and solute transport in UCG surrounding strata and can be further helpful in site selection to avoid the negative environmental impact.

## **6. Conclusions**

The present study aims to address the multiphase flows in the surrounding strata of UCG reactor and to improve the understanding of the potential environmental impact of UCG. For that purpose, a coupled thermal-hydro-chemical (THC) model is employed and developed to investigate the potential gas propagation during the UCG process and solute transport in the UCG decommissioning stage. Based on the verification, validation, and application of the introduced numerical model, the following conclusions can be drawn:

- (1) The gas propagation in strata surrounding the UCG reactor is dominated by rock properties and the produced gas components. In terms of the strata with high air entry value and low permeability, e.g. shale, the gas propagation is limited to the area adjacent to the UCG reactor during the studied period. Besides, the gas propagation is retarded to some extent due to the opposite effect of high pressure on gas diffusion. Based on the improved understanding of the potential syngas migration in coal, the gas escape from one cavity to another can be avoided by choosing the proper width of the safety pillars between the UCG reactors. Moreover, by selecting the target coal seam surrounded by strata layers with high air entry value and low permeability, the reactor can be operated at pressures near

hydrostatic to maximize the methane generation which is favorable under high pressures, and the gas losses from the reactor can be minimized.

- (2) In the strata surrounding the UCG reactor, the propagation of chemicals in aqueous phase with consideration of pure diffusion is limited to 1.0~2.0 m after 10 years. Thereby, the potential negative environmental impact of ash leaching and solute propagation in UCG decommissioning stage can be avoided/minimized by selecting the surrounding strata layers with low permeability.
- (3) The concentrations of gaseous and dissolved chemicals decrease significantly as a result of adsorption on the coal, i.e.,  $\text{CO}_2$  and  $\text{CH}_4$ , phenol and  $\text{NH}_4^+$  can be significantly absorbed by coal. Thereby, the coal seam and strata serve potentially, to some extent, as a natural cleaning system to deal with the chemicals released during and after UCG process. This work also provides further insight into the significance of investigating the adsorption capacities of different rock types to maximize its performance to retard the potential propagation of various chemical species.
- (4) The feasibility of the developed numerical model to study the transport of potential chemicals in both gaseous and aqueous phases during UCG reactor operating process and commissioning stage is well presented. The presented model can be applied in other UCG projects for the preliminary evaluation of their potential environmental impact without considering the disturbed zone along with cavity formation. It will also serve as basis for further investigation to consider the possible thermally/mechanically induced changes in surrounding strata, i.e. porosities, permeabilities, soil water retention properties, and saturation state, during the UCG process.

## **Acknowledgements**

This work was supported by the EU Research Fund for Coal and Steel (RFCS) as a part of the MEGAPlus project (Grant Agreement number 800774-MEGAPlus-RFCS-2017) and the European Regional Development Fund (ERDF) through Welsh Government as a part of the FLEXIS project (Project Reference: 80835). The financial support is gratefully acknowledged.

## **Reference**

Attwood, T., Fung, V., Clark, W.W., 2003. Market opportunities for coal gasification in China. *J. Clean. Prod.* 11, 473–479. [https://doi.org/10.1016/S0959-6526\(02\)00068-9](https://doi.org/10.1016/S0959-6526(02)00068-9)

Bhutto, A.W., Bazmi, A.A., Zahedi, G., 2013. Underground coal gasification: From fundamentals to applications. *Prog. Energy Combust. Sci.* 39, 189–214. <https://doi.org/10.1016/j.pecs.2012.09.004>

Bird, R.B., Stewart, W.E., Lightfoot, E.N., 1960. *Transport Phenomena*. Wiley, New York.

Burton, E., Friedmann, J., Upadhye, R., 2017. *Practices in Underground Coal Gasification*. Lawrence Livermore National Lab, Livermore, CA (United States).

Campbell, J.H., Pellizzari, E., Santor, S., 1978. Results of a groundwater quality study near an underground coal gasification experiment (Hoe Creek I). Lawrence Livermore Laboratory, Livermore, CA (United States). Rept. UCRL-52405.

Chappell, R., Mostade, M., 1998. The EL TREMEDAL underground coal gasification filed test in Spain first trial at great depth and high pressure, in: The Fifteenth Annual International Pittsburgh Coal Conference. Pittsburgh, USA.

Chen, S., Jin, L., Chen, X., 2011. The effect and prediction of temperature on adsorption capability of coal/CH<sub>4</sub>. *Procedia Eng.* 26, 126–131. <https://doi.org/10.1016/j.proeng.2011.11.2149>

Creedy, D.P., Garner, K., Holloway, S., Jones, N., Ren, T.X., 2001. Review of underground coal gasification technological advancements. UK DTI Cleaner Coal Technology Transfer Programme; 2001. COAL R211/Pub URN 01/1041 Contract No.: COAL R211/Pub URN 01/1041.

Dalton, V.A., Campbell, J.H., 1978. Laboratory measurement of groundwater leaching and transport of pollutants produced during underground coal gasification. *In Situ* 2, 295–328.

Derbin, Y., Walker, J., Wanatowski, D., Marshall, A., 2015. Soviet experience of underground coal gasification focusing on surface subsidence. *J. Zhejiang Univ. Sci. A* 16, 839–850. <https://doi.org/10.1631/jzus.A1500013>

Ferrari A., Favero V., Marschall P., Laloui L..2014. Experimental analysis of the water retention behaviour of shales. *Int. J. Rock Mech. Min. Sci.* 72: 61–70. <https://doi.org/10.1016/j.ijrmms.2014.08.011>.

Gainer, J. L., Metzner, A. B., 1965. *AIChE-Chem E Symp. Ser.* 6, 74.

Hosking, L.J., Thomas, H.R., Sedighi, M., 2018. A dual porosity model of high-pressure gas flow for geenergy applications. *Can. Geotech. J.* 55, 839–851. <https://doi.org/10.1139/cgj-2016-0532>

Humenick, M.J., Maitox, C.F., 1977. Groundwater Pollutants From Underground Coal Gasification. *Water Res.* 12, 463–469.

Humenick, M.J., Morgan, J.R., Nolan., B.T., 1987. Adsorption of UCG organics by coal, char, activated char and ash." *In Situ* 11.4.

Imran, M., Kumar, D., Kumar, N., Qayyum, A., Saeed, A., Bhatti, M.S., 2014. Environmental concerns of underground coal gasification. *Renew. Sustain. Energy Rev.* 31, 600–610. <https://doi.org/10.1016/j.rser.2013.12.024>

Jabłońska, B., 2012. Sorption of phenol on rock components occurring in mine drainage water sediments. *Int. J. Miner. Process.* 104–105, 71–79. <https://doi.org/10.1016/j.minpro.2011.12.008>

Jiang, L., Chen, Z., Farouq Ali, S.M., 2020. Thermal-hydro-chemical-mechanical alteration of coal pores in underground coal gasification. *Fuel* 262, 116543. <https://doi.org/10.1016/j.fuel.2019.116543>

Kapusta, K., Stańczyk, K., Wiatowski, M., Chećko, J., 2013. Environmental aspects of a field-scale underground coal gasification trial in a shallow coal seam at the Experimental Mine Barbara in Poland. *Fuel* 113, 196–208. <https://doi.org/10.1016/j.fuel.2013.05.015>

Khadse, A.N., 2015. Resources and economic analyses of underground coal gasification in India. *Fuel* 142, 121–128. <https://doi.org/10.1016/j.fuel.2014.10.057>

Khan, M.M., Mmbaga, J.P., Shirazi, A.S., Trivedi, J., Liu, Q., Gupta, R., 2015. Modelling underground coal gasification-A review. *Energies* 8, 12603–12668. <https://doi.org/10.3390/en8112331>

Kosowska-Golachowska, M., Gajewski, W., Musiał, T., 2014. Determination of the effective thermal conductivity of solid fuels by the laser flash method. *Arch. Thermodyn.* 35, 3–16. <https://doi.org/10.2478/aoter-2014-0018>

Krooss, B.M., Van Bergen, F., Gensterblum, Y., Siemons, N., Pagnier, H.J.M., David, P., 2002. High-pressure methane and carbon dioxide adsorption on dry and moisture-equilibrated Pennsylvanian coals. *Int. J. Coal Geol.* 51, 69–92. [https://doi.org/10.1016/S0166-5162\(02\)00078-2](https://doi.org/10.1016/S0166-5162(02)00078-2)

Liu, G., Smirnov, A.V. Modeling of carbon sequestration in coal-beds: A variable saturated simulation, 2008. *Energy Convers. Manag.* 49: 2849–2858. <https://doi.org/10.1016/j.enconman.2008.03.007>.

Liu, S. qin, Li, J. gang, Mei, M., Dong, D. lin, 2007. Groundwater Pollution from Underground Coal Gasification. *J. China Univ. Min. Technol.* 17, 467–472. [https://doi.org/10.1016/S1006-1266\(07\)60127-8](https://doi.org/10.1016/S1006-1266(07)60127-8)

Man, Y., Yang, S., Xiang, D., Li, X., Qian, Y., 2014. Environmental impact and techno-economic analysis of the coal gasification process with/without CO<sub>2</sub> capture. *J. Clean. Prod.* 71, 59–66. <https://doi.org/10.1016/j.jclepro.2013.12.086>

Mao, F., 2016. Underground coal gasification (UCG): A new trend of supply-side economics of fossil fuels. *Nat. Gas Ind. B* 3, 312–322. <https://doi.org/10.1016/j.ngib.2016.12.007>

Ogata, A., Banks, R.B., 1961. A solution of the differential equation of longitudinal dispersion in porous media: fluid movement in earth materials. US Gov. Print. Off. A1–A7.

Otto, C., Kempka, T., 2015. Thermo-mechanical simulations of rock behavior in underground coal gasification show negligible impact of temperature-dependent parameters on permeability changes. *Energies* 8, 5800–5827. <https://doi.org/10.3390/en8065800>

Parajuli K., Sadeghi M., Jones S.B., 2017. A binary mixing model for characterizing stony-soil water retention. *Agric. For. Meteorol.* 244–245: 1–8. <https://doi.org/10.1016/j.agrformet.2017.05.013>.

Perkins, G., 2018. Underground coal gasification – Part I: Field demonstrations and process performance. *Prog. Energy Combust. Sci.* 67, 158–187. <https://doi.org/10.1016/j.peccs.2018.02.004>

Pillalamarry, M., Harpalani, S., Liu, S., 2011. Gas diffusion behavior of coal and its impact on production from coalbed methane reservoirs. *Int. J. Coal Geol.* 86, 342–348. <https://doi.org/10.1016/j.coal.2011.03.007>

Poling, B.E., Prausnitz, J.M., O'connell, J.P., 2001. *The Properties of Gases and Liquids*. McGraw-hill, New York. <https://doi.org/10.1063/1.3060771>

Pone, J.D.N., Halleck, P.M., Mathews, J.P., 2009. Sorption capacity and sorption kinetic measurements of CO<sub>2</sub> and CH<sub>4</sub> in confined and unconfined bituminous coal. *Energy and Fuels* 23, 4688–4695. <https://doi.org/10.1021/ef9003158>

Sadasivam, S., Zagorščak, R., Thomas, H.R., Kapusta, K., Stańczyk, K., 2020. Characterisation of the Contaminants Generated from a Large-Scale Ex-Situ Underground Coal Gasification Study Using High-Rank Coal from the South Wales Coalfield. *Water. Air. Soil Pollut.* 231, 1–16. <https://doi.org/10.1007/s11270-020-04888-1>

Shafirovich, E., Varma, A., 2009. Underground coal gasification: A brief review of current status. *Ind. Eng. Chem. Res.* 48, 7865–7875. <https://doi.org/10.1021/ie801569r>

Soukup, K., Hejtmánek, V., Čapek, P., Stanczyk, K., Šolcová, O., 2015. Modeling of contaminant migration through porous media after underground coal gasification in shallow coal seam. *Fuel Process. Technol.* 140, 188–197. <https://doi.org/10.1016/j.fuproc.2015.08.033>

Strugała-Wilczek, A., Stańczyk, K., 2016. Leaching behaviour of metals from post-underground coal gasification cavity residues in water differing in mineralization. *Fuel* 173, 106–114. <https://doi.org/10.1016/j.fuel.2016.01.046>

Strugała-Wilczek, A., Stańczyk, K., Bebek, K., 2020. Comparison of Metal Adsorption from Aqueous Solutions on Coal and Char Remaining After In-situ Underground Coal Gasification (UCG). *Mine Water Environ.* 39, 369–379. <https://doi.org/10.1007/s10230-020-00677-8>

Stuermer, D.H., Ng, D.J., Morris, C.J., 1982. Organic Contaminants in Groundwater near an Underground Coal Gasification Site in Northeastern Wyoming. *Environ. Sci. Technol.* 16, 582–587. <https://doi.org/10.1021/es00103a009>

Tang, F., Wang, L., Lu, Y., Yang, X., 2015. Thermophysical properties of coal measure strata under high temperature. *Environ. Earth Sci.* 73, 6009–6018. <https://doi.org/10.1007/s12665-015-4364-0>

Thomas, H.R., 1985. Modelling two - dimensional heat and moisture transfer in unsaturated soils, including gravity effects. *Int. J. Numer. Anal. Methods Geomech.* 9, 573 - 588. <https://doi.org/10.1002/nag.1610090606>

Thomas, H.R., Cleall, P., Li, Y.C., Harris, C., Kern-Luetschg, M., 2009. Modelling of cryogenic processes in permafrost and seasonally frozen soils. *Geotechnique* 59, 173–184. <https://doi.org/10.1680/geot.2009.59.3.173>

Thomas, H.R., He, Y., Onofrei, C., 1998. An examination of the validation of a model of the hydro/thermo/mechanical behaviour of engineered clay barriers. *Int. J. Numer. Anal. Methods Geomech.* 22, 49–71. [https://doi.org/10.1002/\(SICI\)1096-9853\(199801\)22:1<49::AID-NAG908>3.0.CO;2-I](https://doi.org/10.1002/(SICI)1096-9853(199801)22:1<49::AID-NAG908>3.0.CO;2-I)

Tu, Y., Feng, P., Ren, Y., Cao, Z., Wang, R., Xu, Z., 2019. Adsorption of ammonia nitrogen on lignite and its influence on coal water slurry preparation. *Fuel* 238, 34–43. <https://doi.org/10.1016/j.fuel.2018.10.085>

Wang, Y., Liu, S., 2016. Estimation of Pressure-Dependent Diffusive Permeability of Coal Using Methane Diffusion Coefficient: Laboratory Measurements and Modeling. *Energy and Fuels* 30, 8968–8976. <https://doi.org/10.1021/acs.energyfuels.6b01480>

Wen, Z., Yu, Y., Yan, J., 2016. Best available techniques assessment for coal gasification to promote cleaner production based on the ELECTRE-II method. *J. Clean. Prod.* 129, 12–22. <https://doi.org/10.1016/j.jclepro.2016.04.136>

Wiatowski, M., Kapusta, K., Ludwik-Pardała, M., Stańczyk, K., 2016. Ex-situ experimental simulation of hard coal underground gasification at elevated pressure. *Fuel* 184, 401–408. <https://doi.org/10.1016/j.fuel.2016.07.020>

Wu, Y.S., Li, J., Ding, D.Y., Wang, C., Di, Y., 2014. A generalized framework model for the simulation of gas production in unconventional gas reservoirs. *SPE J.* 19, 845–857. <https://doi.org/10.2118/163609-PA>

Wu, Y.S., Pruess, K., Persoff, P., 1998. Gas Flow in Porous Media with Klinkenberg Effects. *Transp. Porous Media* 32, 117–137. <https://doi.org/10.1023/A:1006535211684>

Xie, J., Xin, L., Hu, X., Cheng, W., Liu, W., Wang, Z., 2020. Technical application of safety and cleaner production technology by underground coal gasification in China. *J. Clean. Prod.* 250, 119487. <https://doi.org/10.1016/j.jclepro.2019.119487>

Xin, L., Wang, Z. tang, Wang, G., Nie, W., Zhou, G., Cheng, W. min, Xie, J., 2017. Technological aspects for underground coal gasification in steeply inclined thin coal seams at Zhongliangshan coal mine in China. *Fuel* 191, 486–494. <https://doi.org/10.1016/j.fuel.2016.11.102>

Yang, L., Zhang, X., 2009. Modeling of Contaminant transport in Underground Coal Gasification. *Energy and Fuels* 23, 193–201. <https://doi.org/10.1017/CBO9781107415324.004>

Zagorščak, R., An, N., Palange, R., Green, M., Krishnan, M., Thomas, H.R., 2019. Underground coal gasification – A numerical approach to study the formation of syngas and its reactive transport in the surrounding strata. *Fuel* 253, 349–360. <https://doi.org/10.1016/j.fuel.2019.04.164>

Zagorščak, R., Sedighi, M., Thomas, H.R., 2017. Effects of thermo-osmosis on hydraulic behavior of saturated clays. *Int. J. Geomech.* 17, 1–10. [https://doi.org/10.1061/\(ASCE\)GM.1943-5622.0000742](https://doi.org/10.1061/(ASCE)GM.1943-5622.0000742)

Zagorščak, R., Sadasivam, S., Thomas, H.R., Stańczyk, K. and Kapusta, K., 2020. Experimental study of underground coal gasification (UCG) of a high-rank coal using atmospheric and high-pressure conditions in an ex-situ reactor. *Fuel* 270, 117490. <https://doi.org/10.1016/j.fuel.2020.117490>.

Zhu, W.C., Wei, C.H., Liu, J., Qu, H.Y., Elsworth, D., 2011. A model of coal-gas interaction under variable temperatures. *Int. J. Coal Geol.* 86, 213–221. <https://doi.org/10.1016/j.coal.2011.01.011>

## Table captions

Table 1: Parameters used for COMPASS model validation exercises against laboratory data.

Table 2: Material parameters used for the application of COMPASS model to study gaseous transport in strata surrounding the UCG reactor (Liu and Smirnov, 2008; Ferrari et al., 2014; Parajuli et al., 2017).

Table 3. Average gas concentrations observed in El Tremedal (Spain) UCG trial (Chappell and Mostade, 1998).

Table 4. Schematic of the initial and boundary conditions applied for the gas transport during UCG process and solute transport in UCG decommissioning stage.

Table 5. Adsorption parameters of phenol and  $\text{NH}_4^+$  by coal.

## Figure captions

Figure 1. A schematic of phenomena in the UCG cavity and surrounding strata.

Figure 2. The comparison between the analytical and numerical (COMPASS model) results in terms of (a) solute concentration profiles after 1000 hours and (b) solute concentration breakthrough curve at the point (0.5, 0.1).

Figure 3. Comparison of gas concentration profiles with and without considering adsorption by using the numerical and analytical solutions in a radially infinite system after 1 day.

Figure 4. Schematic diagram of the experimental setup used to simulate ash leaching and solute flow through a coal seam (after Dalton and Campbell, 1978).

Figure 5. Comparison of measured and calculated leachate mass evolution of  $\text{Ca}^{2+}$  during the leachate process

Figure 6. (a) NaBr and (b) phenol breakthrough curves calculated and observed at various distances along a 1.52 m packed coal column.

Figure 7. (a) Soil-water retention characteristics and (b) hydraulic conductivity variations of the porous media (sandstone, coal, and shale).

Figure 8. (a) Degree of saturation and (b) heat propagation in different materials (sandstone, coal and shale) after 10 days.

Figure 9. Gas propagation in different materials after 10 days: (a) sandstone, (b) coal, and (c) shale.

Figure 10. The syngas propagation with and without considering temperature and pressure effects on gas transport in coal during UCG process after 10 days: (a)  $\text{CO}_2$ ,  $\text{CH}_4$  and  $\text{H}_2$ , (b)  $\text{CO}$  and  $\text{H}_2\text{S}$ .

Figure 11. The solutes propagation with and without considering ground water flow in different materials after 10 years: (a) sandstone, (b) coal, and (c) shale.

Figure 12. The propagation of (a) phenol,  $\text{CN}^-$ ,  $\text{NH}_4^+$  and (b)  $\text{Ca}^{2+}$  and  $\text{SO}_4^{2-}$  with and without considering temperature effect in coal after 10 years.

Figure 13. The propagation of (a) phenol and (b)  $\text{NH}_4^+$  with and without considering adsorption in coal after 10 years under the effect of ground flow (case3).

Table 1: Parameters used for COMPASS model validation exercises against laboratory data.

Material parameters	Porosity, n (-)	Diffusion coefficient, D (m <sup>2</sup> /s)	Liquid velocity, V <sub>l</sub> (m/s)	Retardation factor, B
NaBr experiment	0.3	5×10 <sup>-9</sup>	1.25×10 <sup>-6</sup>	1.39
Phenol experiment	0.3	1.94×10 <sup>-7</sup>	3.2×10 <sup>-6</sup>	20.8

Table 2: Material parameters used for the application of COMPASS model to study gaseous transport in strata surrounding the UCG reactor (Liu and Smirnov, 2008; Ferrari et al., 2014; Parajuli et al., 2017).

Parameter	Porosity (-)	Density (kg/m <sup>3</sup> )	Permeability (m <sup>2</sup> )	Van Genuchten (VG) model parameters			
				$\alpha$ (m <sup>-1</sup> )	n	S <sub>r</sub>	S <sub>s</sub>
Sandstone	0.34	2650	1×10 <sup>-15</sup>	1.003	2.798	0.2	0.9
Coal	0.06	1376	1×10 <sup>-16</sup>	1.89	4.8	0.2	0.9
Shale	0.09	2316	1×10 <sup>-17</sup>	7.5×10 <sup>-5</sup>	1.85	0.05	0.9

Table 3. Average gas concentrations observed in El Tremedal (Spain) UCG trial (Chappell and Mostade, 1998).

Gasification experiment	Average process gas concentration, vol. %				
	CO <sub>2</sub>	CH <sub>4</sub>	H <sub>2</sub>	CO	H <sub>2</sub> S
Sub-bituminous coal seam	42.1	13.8	24.9	10.8	8.4

Table 4. Schematic of the initial and boundary conditions applied for the gas transport during UCG process and solute transport in UCG decommissioning stage.

Stage	Injection boundary conditions	Initial conditions	Far-field boundary conditions
(mol/m <sup>3</sup> for gas, ppm for solute)			
During UCG reactor operating stage	C01 = 210.79 (CO <sub>2</sub> )	C <sub>i</sub> = 0.1	C <sub>i</sub> = 0.1
	C02 = 69.09 (CH <sub>4</sub> )	U <sub>0</sub> = 4.8 MPa	U <sub>bc</sub> = 4.8 MPa
	C03 = 124.6 (H <sub>2</sub> )	T <sub>0</sub> = 303.15 K	T <sub>bc</sub> = 303.15 K
	C04 = 54.07 (CO)		
	C05 = 42.06 (H <sub>2</sub> S)		
	T <sub>0</sub> = 303.15 K (<1.3 days)		
	T <sub>0</sub> = 303.15 to 1273.15 K (1.3 to 10 days)		
UCG decommissioning stage	C01 = 450.0 (phenol)	C <sub>i</sub> = 0.1	C <sub>i</sub> = 0.1
	C02 = 290.0 (CN <sup>-</sup> )	T <sub>0</sub> = 303.15 K	T <sub>bc</sub> = 303.15 K
	C03 = 110.0 (Ca <sup>2+</sup> )		
	C04 = 93.0 (NH <sub>4</sub> <sup>+</sup> )		
	C05 = 260.0 (SO <sub>4</sub> <sup>2-</sup> )		
	T <sub>0</sub> = 303.15 K		
Case1 (Pure diffusion)	U <sub>bc</sub> = 4.8 MPa	U <sub>0</sub> = 4.8 MPa	U <sub>bc</sub> = 4.8 MPa
Case 2 (Pure diffusion + advection)	U <sub>bc</sub> = 4.92 MPa	U <sub>0</sub> = 4.8 MPa	U <sub>bc</sub> = 4.8 MPa
Case 3 (Pure diffusion + advection)	U <sub>bc</sub> = 5.04 MPa	U <sub>0</sub> = 4.8 MPa	U <sub>bc</sub> = 4.8 MPa

Table 5. Adsorption parameters of phenol and  $\text{NH}_4^+$  by coal.

	Saturation capacity (mg/g)	Langmuir adsorption constant (L/mg)
Phenol	11.3	0.0127
$\text{NH}_4^+$	2.91	0.0108

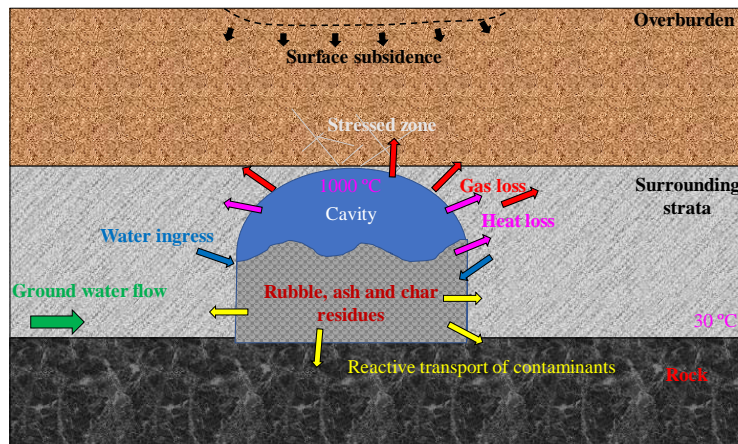


Figure 7. A schematic of phenomena in the UCG cavity and surrounding strata.

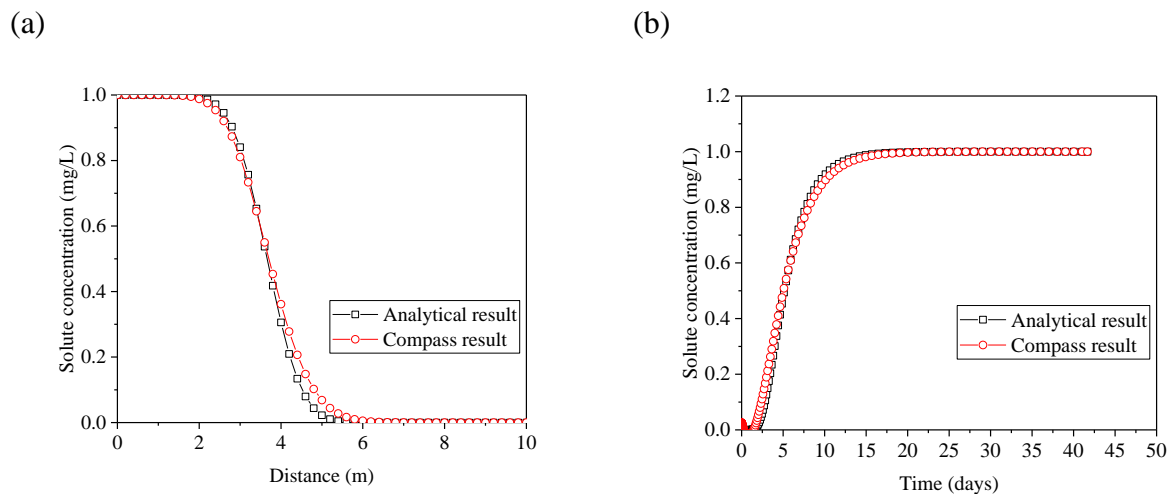


Figure 8. The comparison between the analytical and numerical (COMPASS model) results in terms of (a) solute concentration profiles after 1000 hours and (b) solute concentration breakthrough curve at the point (0.5, 0.1).

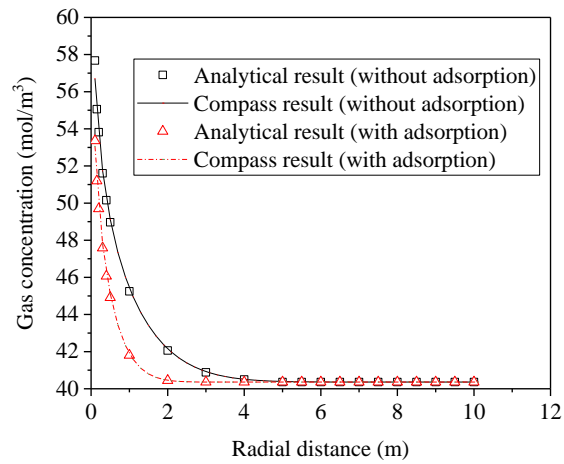


Figure 9. Comparison of gas concentration profiles with and without considering adsorption by using the numerical and analytical solutions in a radially infinite system after 1 day.

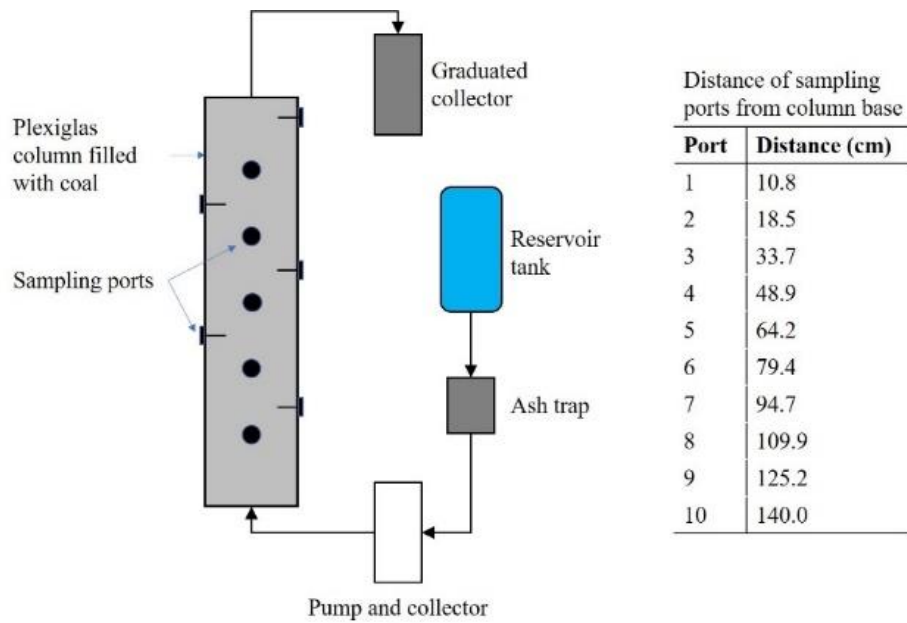


Figure 10. Schematic diagram of the experimental setup used to simulate ash leaching and solute flow through a coal seam (after Dalton and Campbell, 1978).

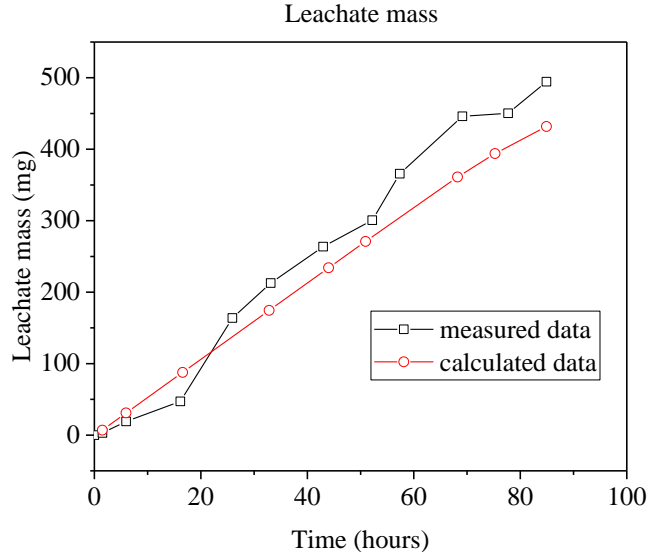


Figure 11. Comparison of measured and calculated leachate mass evolution of  $\text{Ca}^{2+}$  during the leachate process.

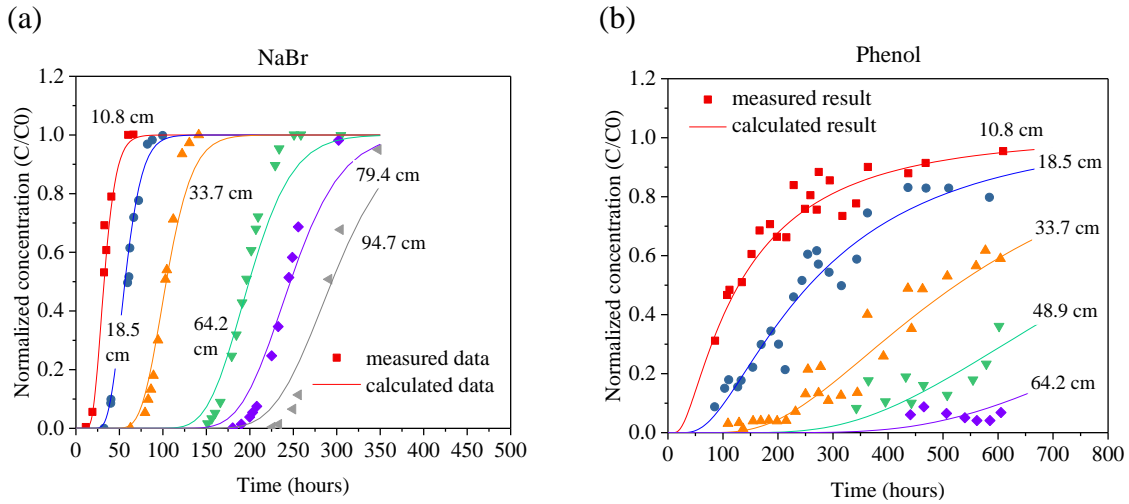


Figure 12. (a) NaBr and (b) phenol breakthrough curves calculated and observed at various distances along a 1.52 m packed coal column.

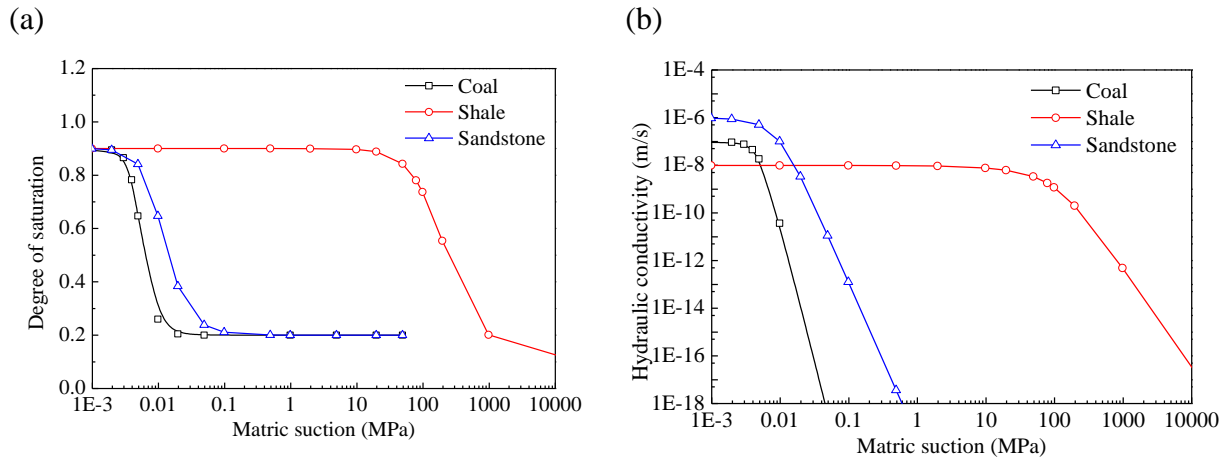


Figure 7. (a) Soil-water retention characteristics and (b) hydraulic conductivity variations of the porous media (sandstone, coal, and shale).

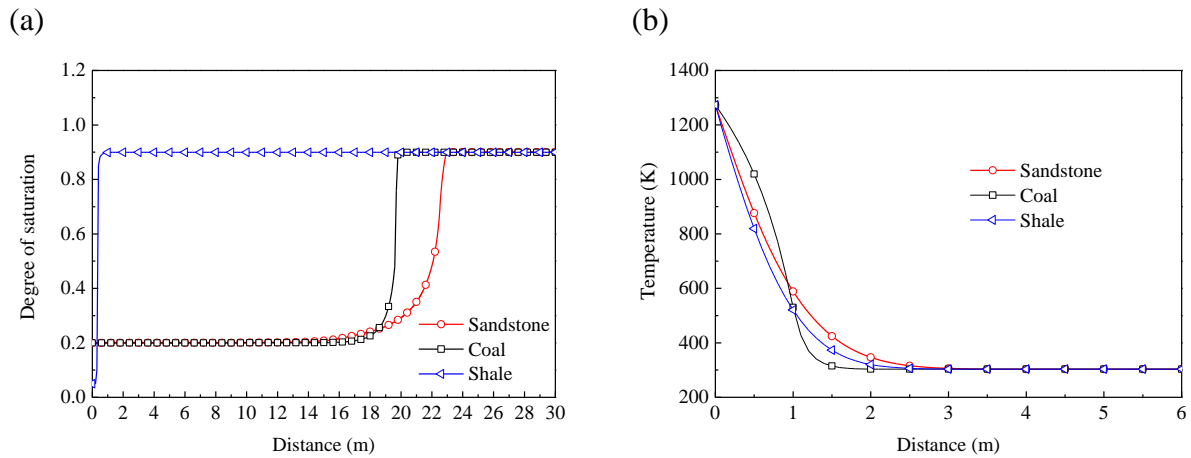


Figure 8. (a) Degree of saturation and (b) heat propagation in different materials (sandstone, coal, and shale) after 10 days.

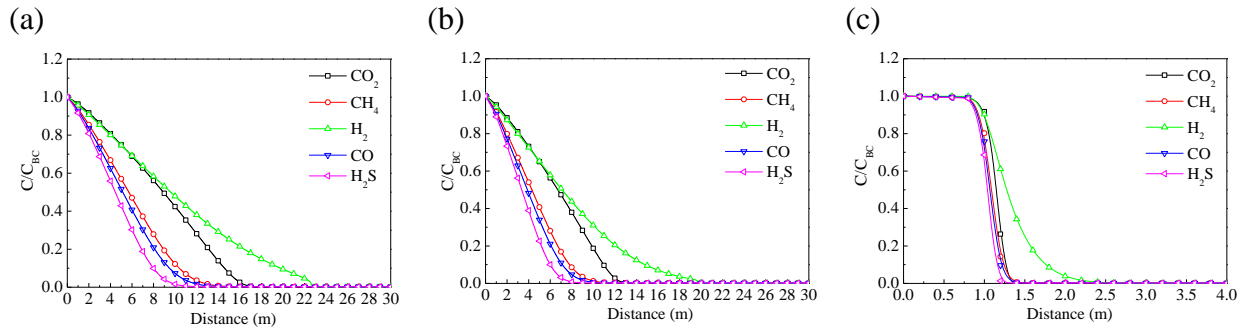


Figure 9. Gas propagation in different materials after 10 days: (a) sandstone, (b) coal, and (c) shale.

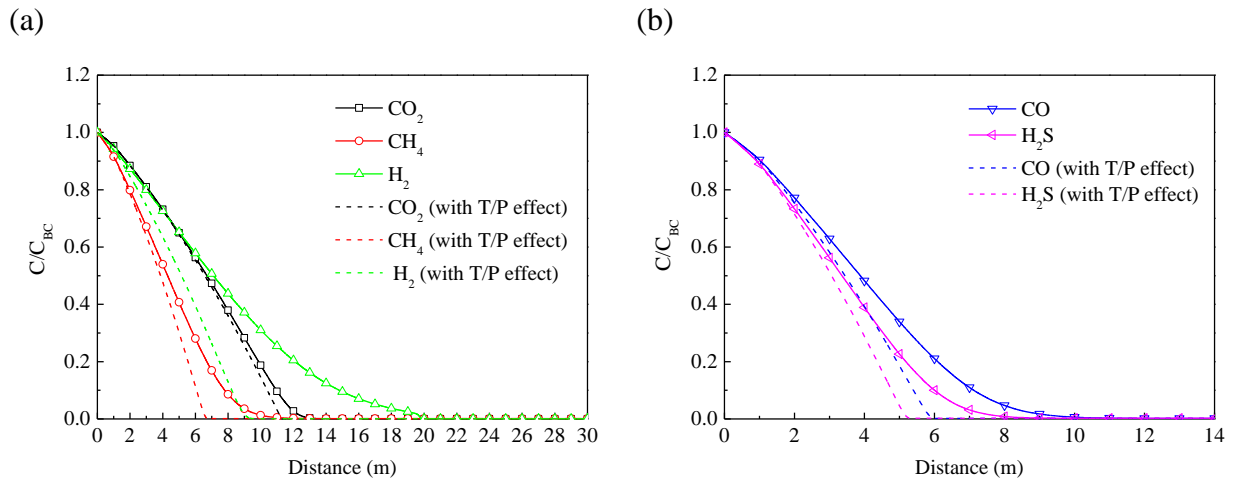


Figure 10. The syngas propagation with and without considering temperature and pressure effects on gas transport in coal during UCG process after 10 days: (a)  $CO_2$ ,  $CH_4$  and  $H_2$ , and (b)  $CO$  and  $H_2S$ .

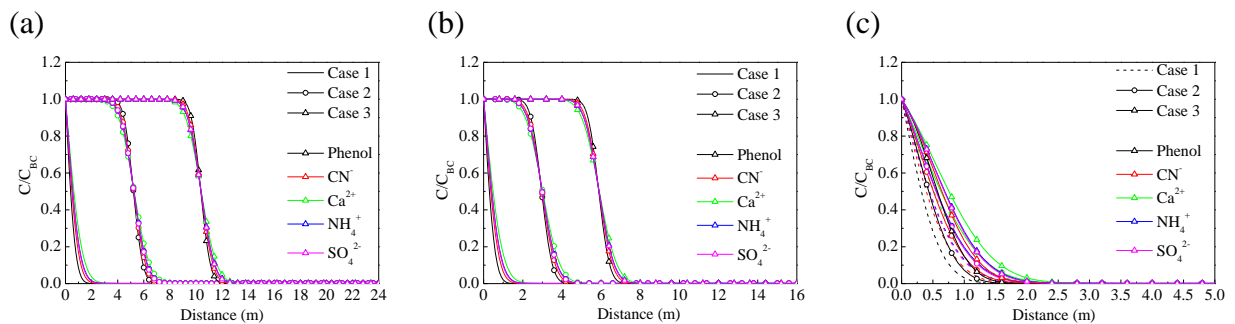


Figure 131. The solutes propagation with and without considering ground water flow in different materials after 10 years: (a) sandstone, (b) coal, and (c) shale.

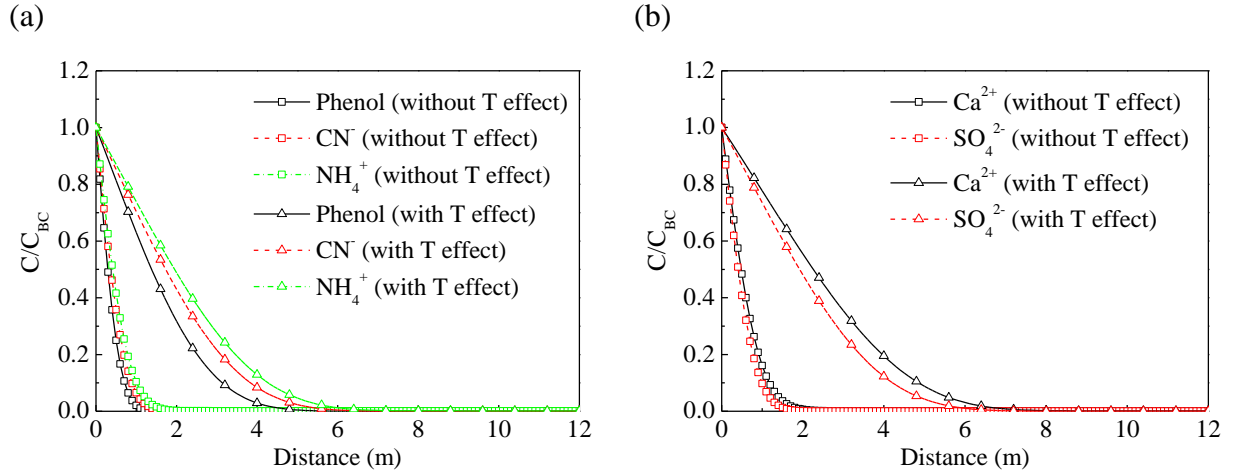


Figure 12. The propagation of (a) phenol,  $\text{CN}^-$ ,  $\text{NH}_4^+$  and (b)  $\text{Ca}^{2+}$  and  $\text{SO}_4^{2-}$  with and without considering temperature effect in coal after 10 years.

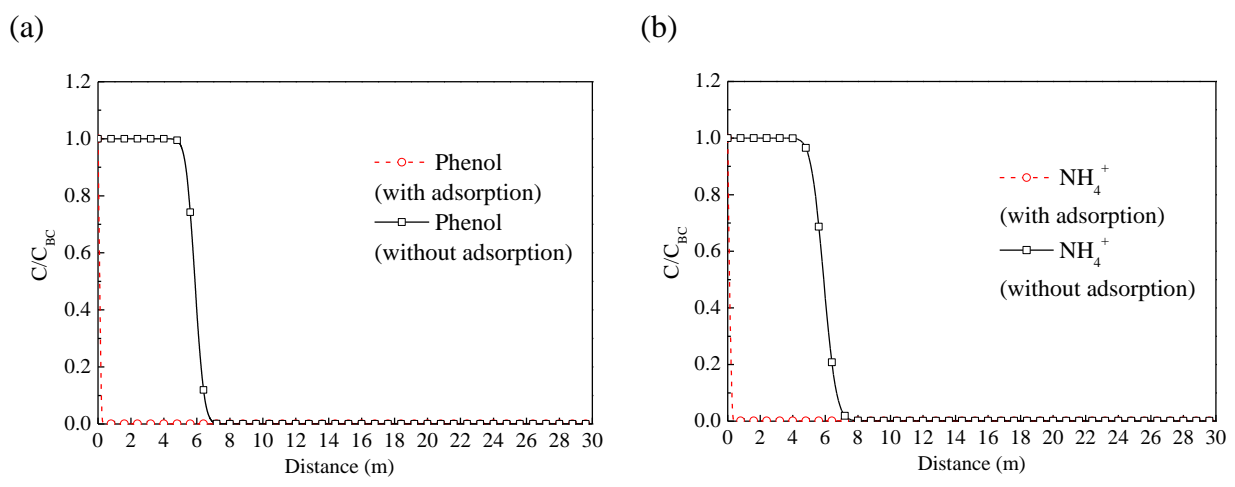


Figure 13. The propagation of (a) phenol and (b)  $\text{NH}_4^+$  with and without considering adsorption in coal after 10 years under the effect of ground flow (case3).